Dynamics of the $FeO^+ + H_2$ Reaction: A Model for Inorganic Oxidation

Stéphanie Essafi,[a] David P. Tew,[a] and Jeremy N. Harvey*[a,b]

Dedication ((optional))

Abstract: Extensive Density Functional Theory (DFT) calculations using the B3LYP functional are used to explore the sextet and quartet energy potential energy surfaces (PESs) of the title reaction, and as a basis to fit global analytical reactive PESs. Surface-hopping dynamics on these PESs reproduces experimentally observed reactivity and confirms that hydrogen activation rather than spin-state change is rate-limiting at low reaction energy, where the main products are $Fe^+ + H_2O$. Spin-state change in the product region is inefficient, so excited-state $^4Fe^+$ is the dominant product. At higher energies, spin-allowed hydrogen atom abstraction to form $FeOH^+$ predominates. At intermediate energy, a previously unexpected rebound mechanism is shown to contribute significantly to reactivity.

The gas-phase reaction between the iron oxide cation FeO^+ and hydrogen has become an important model for many similar oxidation processes in chemistry and biochemistry. As in oxidations by cytochrome P450[1] and iron oxyl complexes,[2] the metal formally transfers an oxygen atom to the co-reactant, with oxidative insertion into the H—H bond leading to formation of water. The process is formally spin-allowed and highly exothermic. The reaction has been studied by a number of mass-spectrometric techniques, which yielded the rate constant from 3 to 670 K as well as the reactive cross-section for collisions occurring at various centre-of-mass energies.[3-5] Interestingly, despite the fact that experimental observations point toward the absence of a significant barrier, the measured rate constant is only about 1% of the Langevin value ($k = 10^{-11}$ cm^3 s^{-1} at 300 K). Other experimental observations are that the rate constant has a negative temperature dependence and that the isotope effect is small. On the theory side, most of the studies have used electronic structure theory methods to compute the energy and structure of the key stationary points involved in the reaction.[6-8] From the beginning, such calculations highlighted a curious observation: the lowest energy pathway from reactants to products involves both sextet and quartet electronic states. Since then, the title reaction has served as a prototype for 'two-state reactivity'.[9]

Static potential energy surface (PES) studies are invaluable but they cannot describe the detailed reaction dynamics, for example they cannot predict the contribution of different pathways to observed reactivity, or the occurrence of non-minimum energy path (MEP) trajectories. Here we report a quasi-classical trajectory study of the title reaction based on new sextet and quartet analytical PESs. The surfaces were parameterized based on DFT calculations using the B3LYP functional for about 30,000 structures up to 200 kcal mol^{-1} above TS1, fitted with an error of less than 2.5 kcal mol^{-1} (see the Methods section and SI for details).

The qualitative features of our calculated PESs (Fig. 1) are very similar to those reported previously. The lowest energy pathway involves formation of an $FeO^+ \bullet H_2$ sextet reactant complex, followed by spin state change through a minimum energy crossing point (MECP1) near the quartet $FeO^+ \bullet H_2$ reactant complex minimum. Dihydrogen activation occurs through the four-membered ring transition state (TS1) and yields the inserted intermediate $[HFeOH]^+$. Still on the quartet surface, this rearranges over the low TS2 to form the product complex $Fe^+ \bullet H_2O$. Dissociation of this complex yields products, with Fe^+ either in its excited quartet state, or in the ground sextet state after a second spin inversion. Spin allowed reaction over sextet TS1 has a higher barrier. Hydrogen atom abstraction leads to $FeOH^+ + H$. The critical point for this process (TS3) can be located on both the sextet and quartet surfaces. For the sextet, it has clear atom transfer character. In the case of the quartet, however, the reaction vector at ^{4}TS3 mostly corresponds to motion of the H_2 moiety towards the oxygen, with the actual bond activation occurring after the TS. Starting from $^4FeO^+$ and H_2, H atom abstraction is barrierless. There is a crossing with the sextet surface near ^{4}TS3, referred to as MECP2. As in previous work, we find direct oxygen insertion into the H—H bond to have a much higher barrier on both spin surfaces.[6]

[a] Dr. S. Essafi, Dr. D. P. Tew, Prof. J. N. Harvey
School of Chemistry
University of Bristol
Cantock's Close, Bristol, BS8 1TS, UK
E-mail: jeremy.harvey@kuleuven.be

[b] Prof. J. N. Harvey
Department of Chemistry
KU Leuven
Celestijnen Laan 200F, B-3001, Heverlee, Belgium

Supporting information for this article is given *via* a link at the end of the document.((Please delete this text if not appropriate))

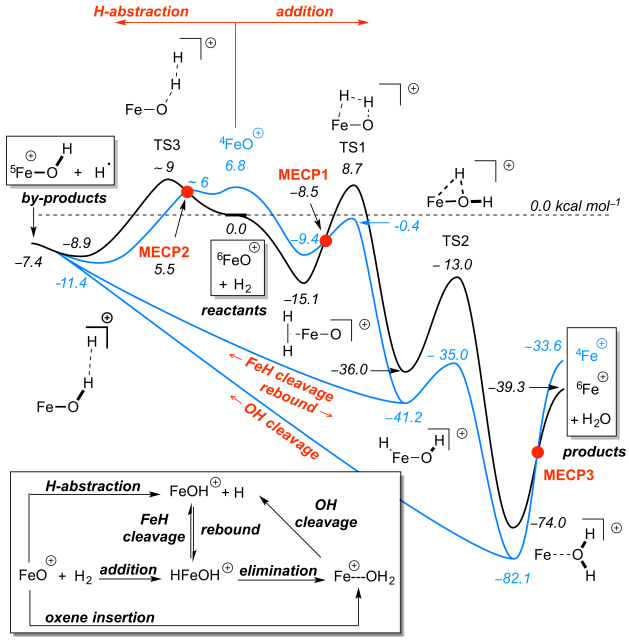

Figure 1. Schematic view of the potential energy surface for the $FeO^+ + H_2$ reaction. The black curve corresponds to the sextet state, the blue one to the lowest quartet state. Energies are in kcal mol^{-1} and relate to the analytical V^{fit}.

Our analytical PESs reproduce the B3LYP optimized structures, harmonic frequencies and energies for key species accurately. Small root-mean-square (RMS) errors of < 0.1 Å for the six interatomic distances, < 150 cm^{-1} for the six frequencies and < 1 kcal mol^{-1} for energies are obtained for most quartet and sextet stationary points (see SI for full details). Some of the largest errors occur on the quartet PES near MECP1 and the $FeO^+ \bullet H_2$ adduct, which can be traced back to the existence of multiple close-lying quartet electronic states that complicate the fitting task in this region. The reaction dynamics samples regions on the PESs that are much higher in energy than the MEPs. To test the accuracy of the fit in such regions, the B3LYP energies were computed at each time step along two typical reactive trajectory paths (see Fig. 2 and Fig. S5). RMS errors of less than 0.7 kcal mol^{-1} were obtained, not much larger than along the MEPs.

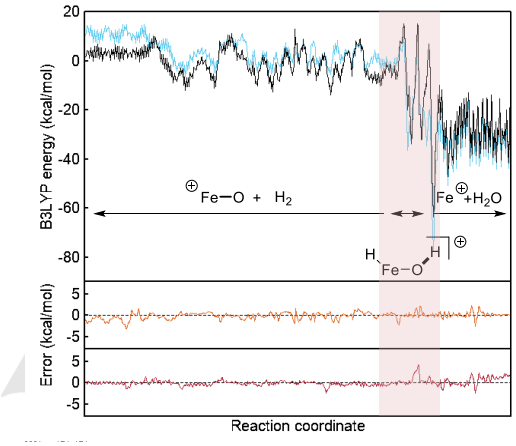

Figure 2. Top part: B3LYP energy along a typical trajectory leading to the product $Fe^+ + H_2O$. Quartet state is shown in blue, sextet state in black. Bottom part: difference between the B3LYP energy and the energy given by the quartet (orange curve; RMSE = 0.55 kcal mol^{-1}, max. deviation = 3.19 kcal mol^{-1}) and sextet (red curve; RMSE = 0.52 kcal mol^{-1}, max. deviation = 4.25 kcal mol^{-1}) analytical PESs for each structure. The highlighted area corresponds to the hydrogen activation phase near TS1.

With efficient and accurate analytical PESs in hand, we turned to study the chemical dynamics of the system. A total of 4.75 million trajectories were propagated starting on the sextet potential with both reactants in their rotational and vibrational ground state, and collision energies ranging between 0.5 and 20 kcal mol^{-1}. Surface-hopping was allowed between sextet and quartet surfaces, with probability derived from spin-orbit coupling matrix elements derived from *ab initio* calculations. Of the 31 thousand reactive trajectories, 3 thousand led to $Fe^+ + H_2O$ and 28 thousand to $FeOH^+ + H$. These were used to compute energy-dependent reactive cross-sections for formation of Fe^+ (σ_{Fe^+}) and $FeOH^+$ (σ_{FeOH^+}) (Fig. 3). Both cross-sections are in reasonably good agreement (within better than a factor of ten) with experimental data obtained for the isotopologous reaction $FeO^+ + D_2$.[3c] In particular, the decrease in cross-section for Fe^+ with increasing collision energy between 0.5 and 5 kcal mol^{-1}, typical of exothermic reactions that are either barrierless or occur over a submerged barrier, is well reproduced. This feature can be explained by the low entropy of the 'tight' TS1 that competes less efficiently with return to reactants for higher collision energies. In the context of the $FeO^+ + H_2$ / D_2 reaction, this behavior was first assumed to be related to the spin-forbidden nature of the reaction.[3a]

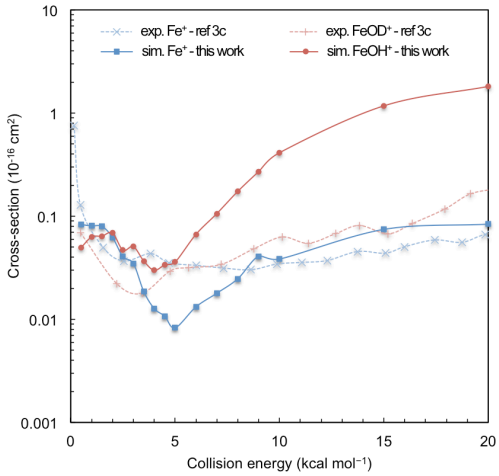

Figure 3. Cross-sections for formation of Fe^+ and $FeOH^+$ as a function of collision energy calculated for the $FeO^+ + H_2$ reaction. Available experimental data for the $FeO^+ + D_2$ reaction are given for comparison.

Let us now discuss the mechanism as it is reproduced by the trajectory calculations in the different energy regimes. At low collision energy (below 4 kcal mol^{-1}), most of the trajectories are

unreactive, as expected given the low cross-section. Except for the largest impact parameters studied here, collision mostly does lead to a recognizable encounter complex $FeO^+•H_2$, but this re-dissociates to reactants. A significant fraction (8% at the lowest energy used, down to 5% for E_{coll} = 4 kcal mol^{-1}) of the trajectories experience at least one hop over[10] onto the quartet surface during the lifetime of the complex. However, still in this energy range, less than 2% of the trajectories that do visit the quartet surface (i.e. roughly 0.1% of the total trajectories) go on to be reactive. The vast majority of them instead revert to the sextet surface and dissociate. Clearly, at these energies, as was found in previous studies,[4,5,7] ^{4}TS1 is the main bottleneck to reaction, with sextet-quartet hopping near MECP1 being faster. After crossing ^{4}TS1 to form ^{4}[HFeOH]$^+$ – the only reactive route that is accessible in this energy regime, referred to here as path A, Fig. 4 – the system rapidly crosses the low ^{4}TS2 to the quartet product complex $^4Fe^+•OH_2$, or decomposes to form H atom and ^{5}FeOH$^+$. The product complex $^4Fe^+•OH_2$ is highly vibrationally excited due to its low potential energy, and dissociates rapidly to yield water and Fe^+. Excited-state $^4Fe^+$ is found to dominate over $^6Fe^+$ (roughly 85:15), as the energy gap between them is relatively small, spin-orbit coupling is very small in this region of the PES, and dissociation is rapid. This ratio of products is consistent with recent experimental observations.[11]

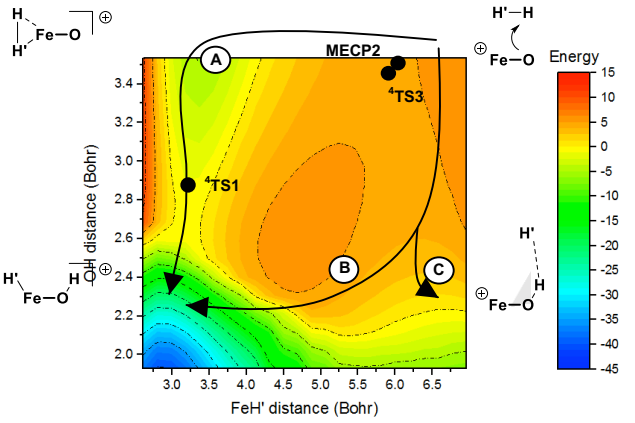

Figure 4. 2D cuts of the B3LYP quartet potential energy surface (kcal mol^{-1}) in the vicinity of ^{4}TS1 obtained from relaxed scans along the O—H and Fe—H' coordinates (*i.e.* insertion of FeO^+ into the H—H' bond). The upper right corner corresponds to the separated reactants, the upper left corner to the adduct complex, the lower left corner to the intermediate [H'FeOH]$^+$, and the lower right corner to [FeOH]$^+$+ H'. ^{4}TS1, ^{4}TS3 and MECP2 are indicated with black circles; MECP1 is out of range.

At intermediate collision energy (between 4 and 9 kcal mol^{-1}), reaction can only occur on the quartet surface, and most trajectories are still unreactive. Spin state change again plays no role in affecting the probability of reacting: roughly 4% of trajectories cross over at least once to the quartet surface, but only 1% of those trajectories go on to react, with the others reverting to reactants. Reaction *via* path A and ^{4}TS1 remains important, but hydrogen atom transfer through ^{4}TS3 is now also possible. Trajectories crossing ^{4}TS3 mostly lead to H + $FeOH^+$ (path C in Fig. 4), accounting for the increasing selectivity in favour of this product in this energy regime. However, the most striking feature of the dynamics, and one that was not expected based on the static *ab initio* PES studies, is path B: between 15 and 25% of all the trajectories crossing ^{4}TS3 lead instead to ^{4}[HFeOH]$^+$, with the second H atom moving (or 'roaming'[12]) around the nascent $FeOH^+$ moiety to form a Fe—H bond, through what is best described as a radical rebound step. The intermediate then react further to form either $Fe^+•H_2O$ through TS2 or $FeOH^+$ + H after homolytic Fe—H bond breaking. It is noticeable that about 15% of the Fe^+ formed in this energy regime derives from this rebound pathway (Fig. 5).

At collision energies above 9 kcal mol^{-1}, reaction on the sextet surface becomes possible, which leads to a large increase in the cross-section. Production of $FeOH^+$ now dominates, with 90% or more of the reactive trajectories. The main route followed is the sextet version of path C, *via* H-abstraction over ^{6}TS3. At 10 kcal mol^{-1}, about half of the Fe^+ ions that are formed originate from path A and ^{4}TS1, with the others formed *via* ^{6}TS1 or *via* sextet or quartet rebound events after TS3. In line with this, the $^4Fe^+$:$^6Fe^+$ ratio is now about 1:1, implying that the spin state of the iron product is determined largely by partitioning into quartet and sextet states in the region of the reaction complex. At higher energies, the role of path A drops still further; at 15 kcal mol^{-1}, less than 10% of the reactive trajectories involve any form of crossing to the quartet surface.

Finally, we note that although trajectories crossing the TS1 or TS3 region can in principle lead to either type of products, there is in practice a strong correlation between the two aspects at intermediate and high collision energy: Fe^+ mostly (> 75 %) comes from trajectories that go through TS1 while $FeOH^+$ comes mostly (> 65 %) from trajectories that go through TS3.

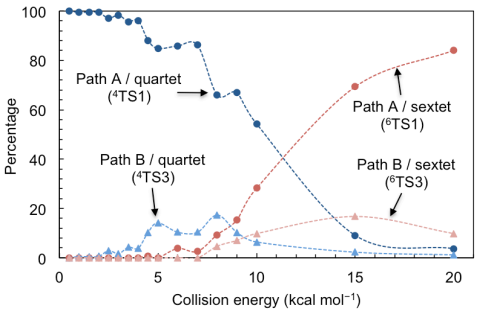

Figure 5. Contribution of the different mechanisms to the production of Fe^+ as a function of collision energy.

In conclusion, we have used very extensive DFT calculations as a basis for fitting analytical PESs for the quartet and sextet electronic states in the FeO^+ + H_2 reaction. This has allowed classical trajectory studies including surface-hopping which yield new insights into the mechanism of this paradigmatic oxidation reaction. Confirming the results of previous *ab initio* and statistical rate theory studies, the main bottleneck to reaction at low energy (relevant for thermal reactivity) is the quartet four-membered cyclic H—H activation ^{4}TS1. Spin-state change in the vicinity of the surface-crossing seam and MECP1 is almost 100 times faster. The trajectory calculations reproduce well the experimentally observed reactive cross-section for forming Fe^+

and $FeOH^+$. The most surprising finding is that at intermediate collision energies, reaction also involves a rebound mechanism with initial homolytic breaking of the H—H bond through TS3 to yield a radical pair $FeOH^+$ + H, and with the H atom then collapsing to form a second O—H bond in $Fe^+ \bullet OH_2$. This simple gas-phase process is an excellent model[13] for many condensed-phase and biological oxidation processes involving iron oxyl active species[1,2]: in these cases, the iron atom has a full ligand shell, which prevents the formation of Fe—H bonds as required by reaction through ^{4}TS1, the dominant process at very low energy in the present reaction. Also, caging by the solvent, enzyme or zeolite environment will lead to much enhanced rebound in those cases compared to the present gas-phase process where $FeOH^+$ is by far the dominant product at higher energies.

Methods

The classical trajectory simulations were performed on analytical quartet and sextet potential energy surfaces fitted to B3LYP/6-311++G(3df,p) energies.[14] For nuclear configurations corresponding to separated reactants $FeO^+ + H_2$ or products $Fe^+ + H_2O$ or $FeOH^+ + H$ ('long-range' part), the analytical potential is obtained as a sum of an intramolecular term and a long-range electrostatic term (charge-induced dipole for reactants, and charge-dipole for $Fe^+ + H_2O$). The intramolecular term was fitted to DFT calculations on the isolated fragments, using a fourth-order Morse-type polynomial as described in the literature.[15] In the reaction region where all atoms are relatively close to one another ('short-range' part), the potential energy is obtained as the sum of a fourth-order Morse polynomial of the six internuclear distances, combined with a correction function that is a sum of distributed four-dimensional Gaussian functions of the internuclear distances.[16] Transition from the long-range to the short-range parts of the potentials is handled by a switching function that smoothly join the two parts. All equations can be found in the SI.

Over 33,000 (sextet) and 26,000 (quartet) B3LYP energies were used in the fit. These correspond to geometries along and around the MEP, and to structures sampled from classical trajectory simulations using early versions of the analytical potential energy surfaces. Two aspects need to be highlighted here: first, there are multiple quartet electronic states fairly close in energy, and great care is needed to converge to the lowest quartet state at each structure.[17] This was ensured through the use of a Fermi-smearing procedure as implemented in Turbomole.[18] Also, the B3LYP functional predicts incorrect relative energies for the ^{6}D and ^{4}F states of Fe^+. Accordingly, the experimental value for this splitting was used in the corresponding long-range part of the quartet potential instead of the DFT splitting.[19]

We used the VENUS program[20] to generate random sets of initial conditions. The starting separation between $^6FeO^+$ and H_2 was set to 15 Å (exceptionally to 10 Å). Reactants were randomly oriented. Reactive trajectories were discarded if the internal energy of H_2O or $FeOH^+$ in the final, separated products, was below their respective zero point energy (13.4 and 7.2 kcal mol^{-1}). We used our own code to propagate trajectories. It uses a standard Velocity-Verlet algorithm coupled to a surface-hopping algorithm[21] of the type 'Fewest Switches' as proposed by Tully.[22] Classical mechanical equations of motion were integrated using a time step of 0.2 fs. A time step of 0.02 fs was used to integrate the quantum mechanical equations. When a switch occurred, the atomic velocities were multiplied by a scalar factor in order to conserve total energy.[23] In case the proposed switch was to a state lying higher in potential energy than the starting state at the point considered, and the change in potential energy was larger than the available nuclear kinetic energies, then no switch was carried out. Finally, we derived spin orbit couplings between sextet and quartet states along the reaction path from matrix elements reported by Danovich and Shaik (see SI for numerical values and further details).[24]

Reactive trajectories were classified a posteriori into four categories depending on the type of H—H bond activation that had taken place (*i.e.* through ^{4}TS1 or ^{6}TS1 or ^{4}TS3 or ^{6}TS3). This was done by monitoring the shortest OH distance and the largest FeH distance.

Acknowledgements

JNH and SE were supported by the EPSRC through grant EP/L005913/1; JNH also acknowledges KU Leuven grant GKF-C9549-C14/15/052. DPT thanks the Royal Society for a University Research Fellowship.

Keywords: iron oxide cation • reaction mechanisms • rebound mechanism • molecular dynamics • surface-hopping

[1] S. Shaik, S. Cohen, Y. Wang, H. Chen, D. Kumar, W. Thiel, *Chem. Rev.* **2010**, *110*, 949–101.

[2] a) S. T. Kleespies, W. N. Oloo, A. Mukherjee, L. Que Jr., *Inorg. Chem.* **2015** *54*, 5053–5064. b) K. Ray, F. F. Pfaff, B. Wang, W. Nam, *J. Am. Chem. Soc.* **2014**, *136*, 13942–13958. c) K. Krebs, D. G. Fujimori, C. T. Walsh, M. Bollinger Jr., *Acc. Chem. Res.* **2007**, *40*, 484–492. d) B. E. R. Snyder, P. Vanelderen, M. L. Bols, S. Hallaert, L. H. Böttger, L. Ungur, K. Pierloot, R. A. Schoonheydt, B. F. Sels, E. I. Solomon, *Nature* 2016, **536**, 317-321.

[3] a) D. Schröder, H. Schwarz, D. E. Clemmer, Y. Chen, P. B. Armentrout, V. I. Baranov, D. K. Bohme, *Int. J. Mass Spectrom. Ion Processes* **1997**, *161*, 175–191. b) D. Schröder, A. Fiedler, M. F. Ryan, H. Schwarz, *J. Phys. Chem.* **1994**, *98*, 68–70. c) D. E. Clemmer, Y.-M. Chen, F. A. Khan, P. B. Armentrout, *J. Phys. Chem.* **1994**, *98*, 6522–6529.

[4] S. G. Ard, J. J. Melko, O. Martinez Jr., V. G. Ushakov, A. Li, R. S. Johnson, N. S. Shuman, H. Guo, J. Troe, A. A. Viggiano, *J. Phys. Chem. A*, **2014**, *118*, 6789–6797.

[5] D. Gerlich, J. Jaík, E. Andris, R. Navrátil, J. Roithová, *Chem. Phys. Chem.* **2016**, *17*, 3723–3739.

[6] M. Filatov, S. Shaik, *J. Phys. Chem. A* **1998**, *102*, 3835–3846.

[7] J. N. Harvey, D. P. Tew, *Int. J. Mass Spectrom.* **2013**, *354–355*, 263–270.

[8] A. Altun, J. Breidung, F. Neese, W. Thiel, *J. Chem. Theory Comput.* **2014**, *10*, 3807–3820.

[9] D. Schröder, S. Shaik, H. Schwarz, *Acc. Chem. Res.* **2000**, *33*, 139–145.

[10] Defined as $p(E_{col}) = \sum_b^{b_{max}} N_{hop}(b) / \sum_b^{b_{max}} N_{tot}(b)$ where $N_{hop}(b)$ is the number of trajectories that hop to the quartet surface at least once at a given impact parameter b and $N_{tot}(b)$ is the total number of trajectories run at this impact parameter.

[11] S. G. Ard, R. S. Johnson, J. J. Melko, O. Martinez Jr., N. S. Shuman, V. G. Ushakov, H. Guo, J. Troe, A. A. Viggiano, *Phys. Chem. Chem. Phys.* **2015**, *17*, 19709–19717.

[12] J. M. Bowman, *Molec. Phys.* **2014**, *112*, 2516-2528.

[13] For a recent review on gas-phase reactions that are models for small molecule activation processes, see H. Schwarz, P. González-Navarrete, J. Li, M. Schlangen, X. Sun, T. Weiske and S. Zhou, *Organometallics* **2017**, *36*, 8-17.

[14] a) P. J. Stephens, F. J. Devlin, C. F. Chabalowski, M. J. Frisch, *J. Phys. Chem.* **1994**, *98*, 11623–11627. b) A. D. Becke, *J. Chem. Phys.* **1993**, *98*, 5648–5652.
[15] B. J. Braams, J. M. Bowman, *Int. Rev. Phys. Chem.* **2009**, *28*, 577–606.
[16] W. Mizukami, S. Habershon, D. P. Tew, *J. Chem. Phys.* **2014**, *141*, 144310.
[17] C. N. Sakellaris, E. Miliordos, A. Mavridis, *J. Chem. Phys.* **2011**, *134*, 234308.
[18] TURBOMOLE V6.6 **2014**, a development of University of Karlsruhe and Forschungszentrum Karlsruhe GmbH, 1989–2007, TURBOMOLE GmbH, since 2007; available from http://www.turbomole.com.
[19] A. Kramida, Yu. Ralchenko, J. Reader, NIST ASD Team (**2015**). *NIST Atomic Spectra Database* (ver. 5.3), [Online]. Available: http://physics.nist.gov/asd [2016, September 23]. National Institute of Standards and Technology, Gaithersburg, MD.
[20] W. L. Hase, R. J. Duchovic, X. Hu, A. Komornicki, K. F. Lim, D.-H. Lu, G. H. Peslherbe, K. N. Swamy, S. R. van de Linde, A. Varandas, H. Wang, R. J. Wolf, VENUS96C, Texas Tech University, Lubbock, TX, **2005**.
[21] For a general overview, see: M. Barbatti, *WIREs Comput Mol Sci.* **2011**, *1*, 620–633.
[22] J. C. Tully, *J. Chem. Phys.* **1990**, *93*, 1061–1071.
[23] R. Schinke, G. C. McBane, *J. Chem. Phys.* **2010**, *132*, 044305.
[24] D. Danovich, S. Shaik, *J. am. Chem. Soc.* **1997**, *119*, 1773–1786.

Entry for the Table of Contents (Please choose one layout)

Layout 1:

COMMUNICATION

On the Rebound:
The reaction of FeO^+ cation with H_2, a simple model for many oxidation processes, involves 'rebound' as well as the known insertion – elimination mechanism, based on classical trajectory studies.

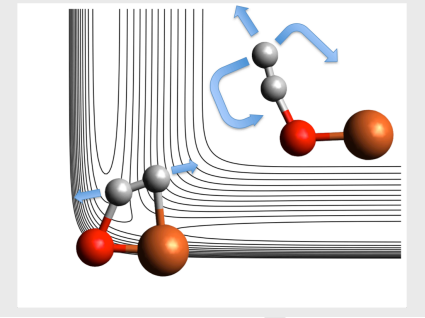

*Essafi, Tew, Harvey**

Page No. – Page No.
Dynamics of the $FeO^+ + H_2$ Reaction: A Model for Inorganic Oxidation

Layout 2:

COMMUNICATION

((Insert TOC Graphic here))

*Author(s), Corresponding Author(s)**

Page No. – Page No.

Title

Text for Table of Contents